Activation of CO_2 by supported Cu Clusters

Satish Kumar Iyemperumal and N. Aaron Deskins

Department of Chemical Engineering, Worcester Polytechnic Institute, 100 Institute Road, Worcester, Massachusetts 01609, USA

1 Effect of TiO_2 Slab Thickness

We tested the effect of the TiO_2 slab thickness as given in Table S1. We modeled a single Cu atom adsorbed in the bridge site between two O_{2c} atoms, and the adsorption energy changed by only 0.08 eV between six and eight layer slabs. Adsorption energies for linear and bent CO_2 molecules over pure TiO_2 changed by $\leq$ 0.03 eV between six and eight layer slabs. We thus used a six layer slab in all of our work.

Table S1: Effect of TiO_2 slab thickness on the adsorption energies (in eV) of a Cu atom, linear CO_2, and bent CO_2. See main text for geometries.

	6 Layers	**8 Layers**
Cu	-2.56	-2.64
CO_2 linear	-0.40	-0.43
CO_2 bent	-0.15	-0.14

2 Comparison of DDEC6 charges with Bader charges

We used DDEC6 charge analysis[1,2] in the present work as the DDEC6 code provides reference core charge densities that are easily augmented with the valence electron densities generated from CP2K. Core densities are necessary to ensure that proper charges on atoms are calculated. DDEC6 iteratively calculates partial atomic charges from the ground state electron density while simultaneously accurately reproducing electrostatic potentials from the electron density of the system.[2] The challenge for any charge analysis technique is that there is no unique way to define atomic charge. Another complication is that calculated charges may not match formal charges due to ionocovalent bonding or limitations of the charge analysis technique. For example, Ti and O atoms in bulk TiO_2 anatase have DDEC6 charges of +2.28 and -1.14, respectively. Formally Ti has a +4 charge, while O has a -2 charge. We note however that the oxidation state of Ti and O in TiO_2 has been recently suggested to be rather +3 and -1.5,[3] in contrast to the traditionally assigned charges in TiO_2.

Nevertheless, charge analysis can provide useful insight on charge transfer during an adsorption process. Another widely used method is Bader charge analysis,[4,5] where the electron density of a material is partitioned by determining the zero flux surfaces around each atom. We compared the charges calculated from DDEC6 with Bader for several molecules like CO_2, CO_2-, CO, O_2, OH, and OH^-, as well as periodic solid systems like CO_2, $LiTiO_2$, $LiTi_2O_4$, CuO, and Cu_2O in Table S2. We show in this table also results calculated using a common periodic DFT code, VASP.[6,7] For the bulk crystals, calculated charges using DDEC6+CP2K and Bader+VASP gave a mean absolute difference of 0.08 e^-. For molecules, the mean absolute difference was 0.43 e^-. For determining trends in charge transfer the DDEC6 method is fully adequate.

Table S2: DDEC6 and Bader charges calculated using CP2K and VASP for bulk and molecular systems.

	System	Atoms	CP2K + DDEC6	VASP + DDEC6	VASP + Bader
	TiO_2 anatase	Ti	2.28	2.25	2.16
		O	-1.14	-1.12	-1.08
	$LiTiO_2$	Li	0.87	0.89	0.89
		Ti	1.73	1.65	1.57
		O	-1.30	-1.27	-1.23
Bulk	$LiTi_2O_4$	Li	0.90	0.90	0.91
		Ti	1.95	1.94	1.84
		O	-1.20	-1.19	-1.15
	CuO	Cu	0.94	0.94	1.00
		O	-0.94	-0.94	-0.99
	Cu_2O	Cu	0.33	0.33	0.54
		O	-0.65	-0.66	-1.08
	CO_2	C	0.71	0.71	2.01
		O	-0.35	-0.35	-0.99
	CO_2^-	C	0.21	0.28	1.50
		O	-0.61	-0.64	-1.18
	CO	C	0.11	0.11	1.03
		O	-0.11	-0.11	-1.00
	O_2	O	0.00	0.00	-0.05/0.07
	OH	O	-0.33	-0.33	-0.59
		H	0.33	0.33	0.61
Molecules	OH-	O	-1.20	-1.21	-1.46
		H	0.20	0.21	0.51
	CuO	Cu	0.44	0.46	0.59
		O	-0.44	-0.46	-0.55
	Cu_2O	Cu	0.28	0.28	0.44
		O	-0.59	-0.56	-0.81
	Cu_3O	Cu	0.16	0.16	0.32
		O	-0.50	-0.49	-0.85
	CuO_2	Cu	0.59	0.70	0.99
		O	-0.30	-0.35	-0.48

3 Vibrational Frequency Calculations

We determined the effect of several simulation parameters on the vibrational frequency calculations of CO adsorbed on Cu/TiO_2, and linear/bent CO_2 on TiO_2 surfaces. These include the plane wave cutoff energies, number of relaxed (unfrozen) atoms, and step size for displacement when calculating energies/forces. Vibrational frequencies were calculated numerically by displacing atoms to calculate second derivatives. Higher cutoff energies give more accurate energies since the basis set is more complete but require more time. Our strategy involved low/high cutoff energies (300/600 Ry). Because these systems were rather large and we did use large cutoff energies, we selectively froze atoms beyond the adsorption site in order to ensure the vibrational calculations were manageable. Frozen atoms were typically 6-7 Å away from the C atom at the adsorption site. This resulted in a smaller set of atoms displaced during vibrational frequency calculation (in the range of 40-50 atoms), but allowed the atoms that could more directly influence the CO/CO_2 frequencies to affect calculation of the second derivatives. Our tests determined appropriate cutoff energies as well as the number of atoms that should be relaxed in order to obtain reasonable frequencies.

As shown in Table S3, geometry optimization at the higher cutoff energies of 600 Ry followed by a vibrational frequency calculations at 600 Ry were required to obtain accurate frequencies close to the earlier reported experimental and DFT calculated frequencies. For instance, linear CO_2 adsorbed on TiO_2 was calculated to have vibrational frequencies of 2367 (asymmetric stretch) and 1351 (symmetric stretch), which agree well with both previous experimental (2355 and 1379 cm^{-1}) and DFT (2373 and 1323 cm^{-1}) values. We found that relaxing 40-50 atoms around the adsorption site was sufficient to obtain vibrational frequencies that were similar to the values obtained by relaxing one or two layers of TiO_2 slab. For instance, the difference in vibrational frequencies for adsorbed CO with the relaxed number of atoms being 42

atoms and 98 atoms (96 atoms relaxed in the top two layers of the slab and 2 atoms of CO) was only 5 cm^{-1}. We thus relaxed 40-50 atoms around the adsorption site for all our reported frequencies in the main text. With respect to the step size during the finite difference approach, we used $1.0E^{-3}$ Bohr. Tests between $1.0E^{-3}$ and $1.0E^{-2}$ Bohr for CO_2 bent/linear adsorption showed the mean absolute difference to be small (12 cm^{-1}) for adsorbed CO_2 vibrational frequencies. The final settings we used for vibrational calculations were a cutoff of 600Ry, relaxing 40-50 atoms around adsorption site, a step size of $1.0E^{-3}$ Bohr, and a tighter electronic convergence criteria of $1.0E^{-7}$ Hartree. Using these settings the mean absolute difference between our DFT calculated and experimental gas phase CO_2 and CO frequencies were 12 cm^{-1} and 5 cm^{-1} respectively.[8] Our DFT values for linearly adsorbed CO_2 were in good agreement with the experimental values,[9] with a mean absolute difference of 20 cm^{-1} for the asymmetric and symmetric stretching modes.

Table S3: Effect of cutoff energy, number of relaxed atoms during frequency calculations ($N_{relaxed}$) and step size on calculated frequencies. All calculations for adsorbed CO_2 were on pure TiO_2 surfaces, while adsorbed CO were on Cu/TiO_2 surfaces. * indicates the experimentally observed Fermi resonance that shifts the bending frequency to a higher 1271 cm^{-1} value.[10,11] This resonance is not correctly described by the DFT calculations.

	Geo. Opt. Cutoff (Ry)	**Vib. Freq. Cutoff (Ry)**	**$N_{relaxed}$**	**Step Size (Bohr)**	**Frequency (cm^{-1})**
CO (gas)	600	600	2	1.0E-3	2178
Experimental Reference[8]	—	—	—	—	2169
	300	600	98	$1.0E^{-3}$	2072
Adsorbed CO	600	600	98	$1.0E^{-3}$	2102
	600	600	42	1.0E-3	2097
CO_2 (gas)	600	600	3	$1.0E^{-3}$	2358, 1300, 664, 664
Theoretical Reference[12]	—	—	—	—	2365, 1318, 633, 633
Experimental Reference[8]	—	—	—	—	2349, 1333, 667, 667
	300	600	195	$1.0E^{-3}$	2371, 1337, 673, 657
	300	600	99	$1.0E^{-3}$	2372, 1335, 674, 642
Linear CO_2	600	600	42	1.0E-3	2367, 1351, 667, 688
	600	600	42	$1.0E^{-2}$	2370, 1349, 656, 650
Theoretical Reference[12]	—	—	—	—	2373, 1323, 615, 611
Experimental Reference[9]	—	—	—	—	2355, 1379, 1271*
	300	600	195	$1.0E^{-3}$	1730, 1260, 790, 875
	300	600	99	$1.0E^{-3}$	1731, 1260, 791, 872
Bent CO_2	600	600	43	$1.0E^{-3}$	1709, 1277, 822, 718
	600	600	43	$1.0E^{-2}$	1700, 1273, 801, 725
Theoretical Reference[12]	—	—	—		1719, 1249, 785, 730

4 Most Stable Spin State

We calculated the most stable spin state of both gas phase Cu_x clusters and adsorbed Cu_x/TiO_2 geometries. We find that in all the cases, the lowest spin state with minimum number of unpaired electrons (multiplicity of 1 or 2) are the most stable spin state as shown in Table S4.

Table S4: Relative energies (in eV) with respect to the most stable spin state. Zero relative energy correspond to most stable spin state.

	Cu_1	**Cu_3**	**Cu_1/TiO_2**	**Cu_3/TiO_2**
Multiplicity 2	0.00	0.00	0.00	0.00
Multiplicity 4	5.27	1.16	0.85	1.31
	Cu_2	**Cu_4**	**Cu_2/TiO_2**	**Cu_4/TiO_2**
Multiplicity 1	0.00	0.00	0.00	0.00
Multiplicity 3	1.58	0.61	0.43	0.02

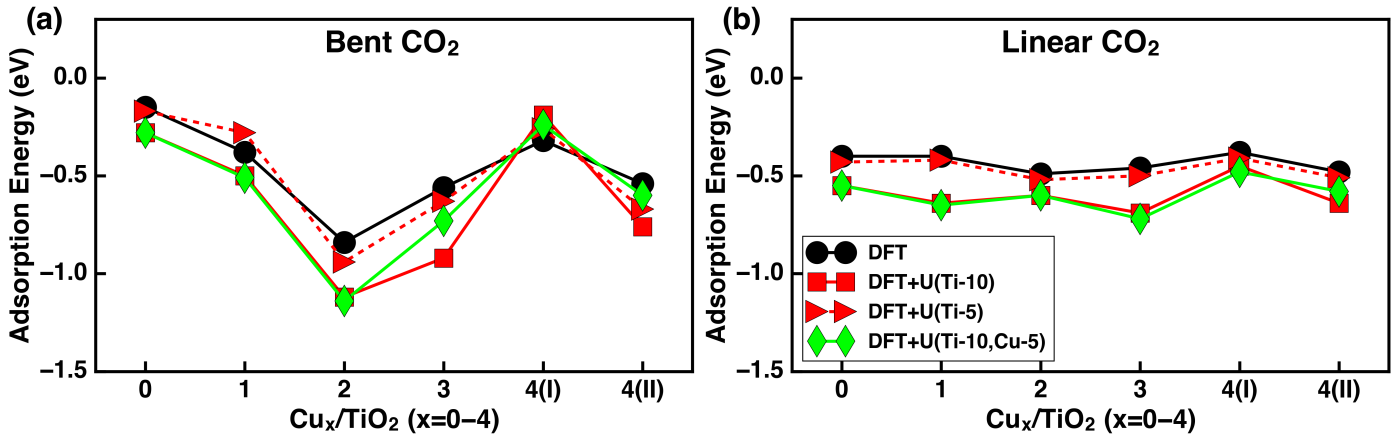

Figure S1: Effect of different U corrections on the adsorption energies of most stable (as discussed in the main text) bent (a) and linear (b) CO_2 adsorption configurations on Cu_x/TiO_2. Shown are results for pure DFT and DFT with U corrections. For example, U(Ti-10,Cu-5) represents a U correction of 10.0 eV applied to Ti and 5.0 eV applied Cu atoms.

5 Effect of DFT+U

5.1 Effect of the U Correction on Adsorption Energies

DFT+U has become a standard way to correct self interaction errors inherent in DFT using generalized gradient approximation exchange-correlation functionals.[13] Earlier DFT studies showed that the effect of U correction on the adsorption energies of adsorbates like formaldehyde or methanol on $CeO_2(111)$,[14] oxygen molecule on TiO_2 rutile (110),[15] and Au_{20}/TiO_2 rutile(110)[16] was small (less than 0.1 eV). However, Garcia and Deskins[17] reported that the adsorption of O_2 on the anatase TiO_2 (101) with oxygen vacancy was strongly destabilized (∼0.8 eV) with increasing U value of up to 10 eV. In the case of adsorption of CO_2, He et al.[18] showed that the energy to convert linear CO_2 to bent CO_2 on the anatase TiO_2 (101) surface differed by only 0.03 eV between DFT and DFT+U (U=4.5 eV). One complication is that the appropriate U value choice depends on the basis set, pseudopotential, the target property (adsorption energy in our case), and the catalyst under consideration. We thus used various U values to determine the DFT+U effect on O_{2c} adsorption over Cu_x/TiO_2 catalysts.

We used three different DFT+U schemes: a U correction (U values reported here are effective U, U_{eff} = U - J) applied to just Ti (5.0 eV), U correction applied to just Ti (10.0 eV), and U corrections applied to both Ti (10.0 eV) and Cu (5.0 eV). All corrections were applied to d electrons. Similar large U values were earlier used in modeling TiO_2 using CP2K.[16,17,19] In the case of Cu, literature suggests that the application of U to Cu atoms in different oxidation states such as in CuO, Cu_2O, and Cu_4O_3 can be challenging.[20,21] Electronic properties such as the band gap of Cu_4O_3 and CuO, direct or indirect band gap in Cu_2O, and location of defect levels in defective bulk Cu_2O were reported to be incorrectly described by DFT+U techniques.[20–22] Nonetheless, in order to test the effect of U on Cu, we chose a representative U value for Cu as 5.0 eV, which is similar to the value of 5.2 eV used earlier.[22,23]

We found that DFT+U predominantly gives more negative adsorption energies compared to DFT as Figure 1 shows. The exception is bent CO_2 on the Cu4(I) structure, where inclusion of U resulted in slight (by less than around 0.1 eV) endothermic adsorption energies compared to the DFT value. The difference between DFT and DFT+U for both bent and linear CO_2 adsorption was small (up to 0.1 eV) when U of 5 eV was applied to Ti, while it was larger (in the range of 0.1 to 0.4 eV) when a U value of 10 eV was applied. Applying a U correction to Cu had almost no effect on bent CO_2 adsorption energies when compared to U of 10 eV applied to Ti, except for the Cu_3 and Cu_4(II) clusters. These clusters where less stable by 0.19 eV, Cu_3, and 0.16 eV, Cu_4(II), when the U correction was also applied to Cu. Only in the case of Cu_4(II) did applying the U correction to Cu have an effect in destabilizing adsorbed linear CO_2, although the effect appears small (0.06 eV). It appears therefore that DFT+U may only meaningfully affect the nature of larger Cu clusters, although this effect is small for the clusters we used. In the case of Cu_4(I), DFT+U results showed that bent CO_2 adsorption is 0.15-0.26 eV less stable than linear CO_2, while DFT results showed this difference between bent and linear CO_2 adsorption to be 0.06 eV. The trends in adsorption energies however are similar regardless of U value choice. Our calculated DFT adsorption energies agree with the literature values. The linear and bent CO_2 adsorption energies reported earlier using DFT[12] were -0.48 eV and -0.01 eV, which are close to our DFT values of -0.40 and -0.15 eV respectively. We therefore present only the DFT adsorption energies in the main text.

5.2 Effect of U Correction on Atomic Charges

We also calculated DDEC6 charges of adsorbed CO_2, as well as Cu_x clusters with and without adsorbed CO_2 using DFT and DFT+U (U of 10 eV on Ti atoms). We found that the DDEC6 charges were predominantly weakly affected (<0.1 electrons) when U corrections are applied (see Table S5). For instance, Cu_3 and Cu_4/TiO_2 charges before CO_2 adsorption were almost the same. The only considerable difference between DFT and DFT+U results was for the case of a single Cu atom. When linear CO_2 was adsorbed, the charge of the Cu atom from DFT was 0.48, compared to 0.65 using DFT+U. When bent CO_2 was adsorbed, the charge of the Cu atom from DFT was 0.59, compared to 0.82 using DFT+U. Otherwise, most charges were similar between DFT and DFT+U. The mean absolute difference in CO_2 charges between DFT and DFT+U was 0.08 electrons. The mean absolute differences in Cu charges between DFT and DFT+U was 0.08 electrons (no CO_2 adsorbed) and 0.13 electrons (CO_2 adsorbed). DFT charges are therefore presented in the main text.

Table S5: DDEC6 charges of linear/bent CO_2 and Cu atoms using the DFT and DFT+U methods. Here, a U correction of 10 eV was applied to the Ti 3d electrons.

No. Cu atoms (Cu_x/TiO_2)	**CO_2 Geometry**	**C, O, O Charges**	**Cu_x Charges (Before Adsorption)**	**Cu_x Charges (After Adsorption)**
DFT Results				
	CO_2 (gas)	0.70,-0.35,-0.35	–	–
0	linear	0.75, -0.31, -0.37	–	–
	bent	0.79,-0.55, -0.54	–	–
1	linear	0.78, -0.40, -0.32	0.53	0.48
	bent	0.79, -0.58, -0.52	–	0.59
2	linear	0.77, -0.40, -0.33	0.13, -0.07	0.13, -0.06
	bent	0.33, -0.53, -0.36	–	0.29, 0.30
3	linear	0.75, -0.29, -0.32	0.24, 0.24, 0.03	0.18, 0.23, -0.01
	bent	0.86, -0.59, -0.45	–	0.16, 0.15, 0.04
4(I)	linear	0.76, -0.32, -0.38	0.52, 0.20, 0.23, -0.07	0.52, 0.21, 0.23, -0.08
	bent	0.83, -0.52, -0.43	–	0.51, 0.16, 0.27, -0.08
4(II)	linear	0.76, -0.33, -0.30	0.42, 0.12, 0.45, -0.06	0.38, 0.10, 0.46, -0.07
	bent	0.82, -0.58, -0.43	–	0.39, -0.01, 0.15, 0.41
DFT+U Results				
0	Linear	0.79, -0.30, -0.42	–	–
	Bent	0.82, -0.58, -0.58	–	–
1	Linear	0.80, -0.43, -0.31	0.58	0.65
	Bent	0.83, -0.65, -0.55	–	0.82
2	Linear	0.80, -0.42, -0.32	0.10, -0.15	0.10, -0.16
	Bent	0.36, -0.61, -0.36	–	0.27, 0.23
3	Linear	0.77, -0.32, -0.39	0.27, 0.27, 0.03	0.27, 0.22, 0.00
	Bent	0.89, -0.61, -0.44	–	0.18, 0.28, 0.01
4(I)	Linear	0.77, -0.31, -0.39	0.50, 0.18, 0.21, -0.10	0.50, 0.19, 0.21, -0.12
	Bent	0.85, -0.53, -0.41	–	0.48, 0.16, 0.24, -0.14
4(II)	Linear	0.77, -0.34, -0.29	0.41, 0.07, 0.44, -0.07	0.37, 0.06, 0.45, -0.10
	Bent	0.84, -0.64, -0.41	–	0.39, 0.15, 0.34, -0.02

5.3 Effect of the U Correction on Electronic States

We also determined how U value choice impacts the electronic structure by examining the density of states of adsorbed Cu at different U values. Yan et al. reported that the significant Cu states are present at the valence band maximum edge.[24] We find that a U value of 5.0 eV applied to Ti describes the Cu/TiO_2 electronic states correctly similar to what Yan et al. have reported and also gives a reasonable band gap of 1.66 eV (see Figure 2). A large U value of 10 eV applied to Ti resulted in Cu states pushed to lower (more negative) energies within the valence band, which is not agreement with previous literature.[24] We thus used a U correction of 5.0 eV to Ti for all our density of states calculations.

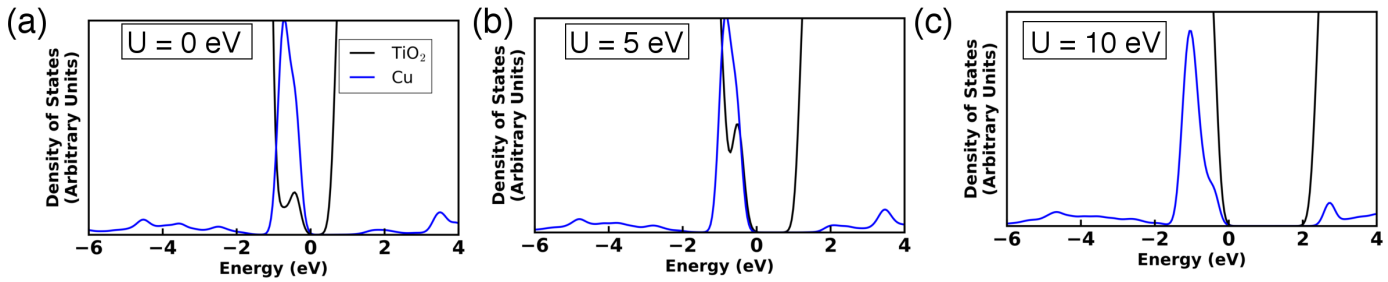

Figure S2: Sited-projected density of states (DOS) for Cu/TiO_2 calculated using U values of 0, 5, and 10 eV (all applied to Ti). The valence band edge for each system has been set to 0 eV in the plots.

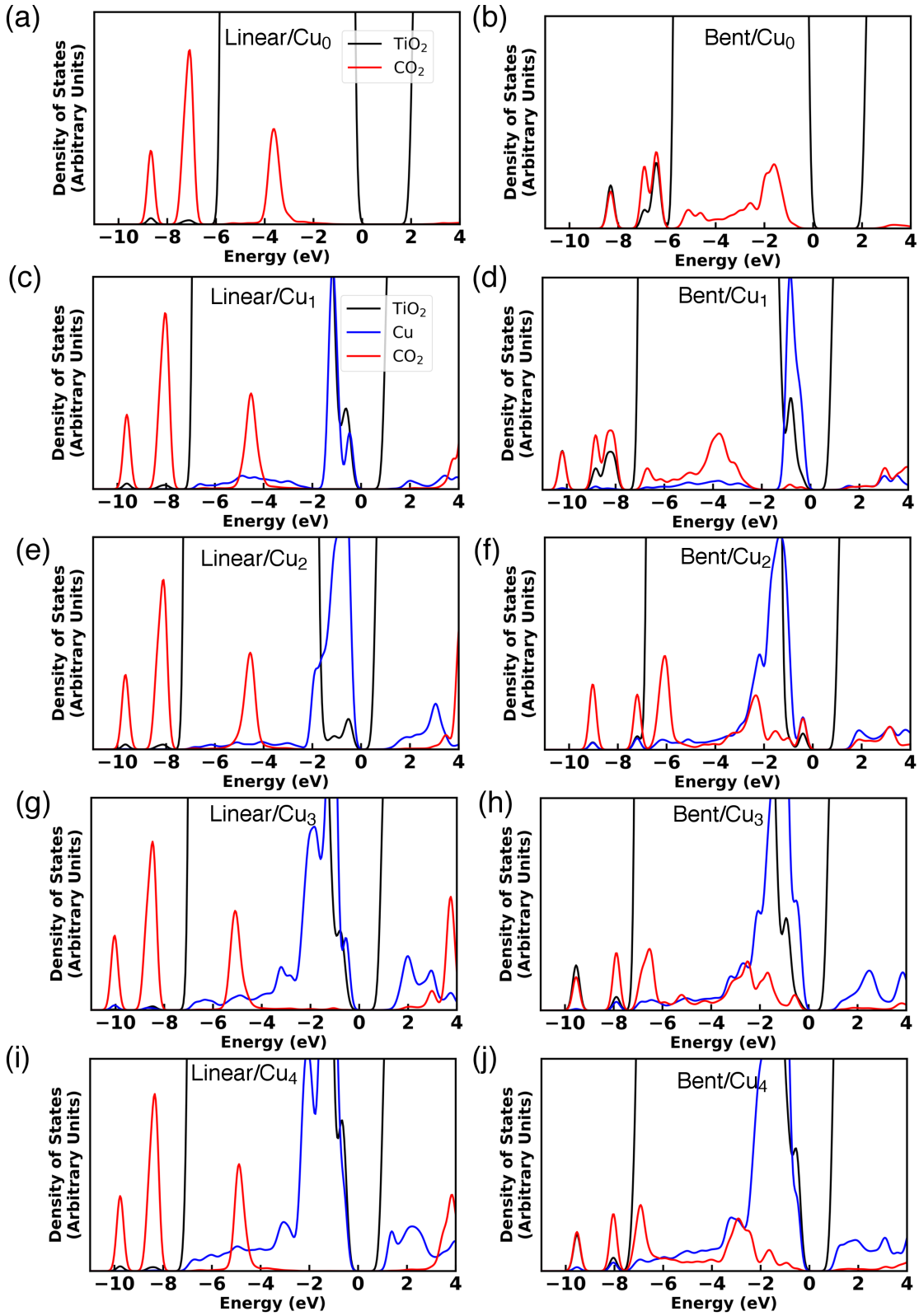

Figure S3: Sited-projected density of states (DOS) for linear and bent CO_2 adsorbed on Cu_x/TiO_2 for a U value of 5 eV applied to Ti. The left plots show linear CO_2 while the right plots show bent CO_2. The valence band edge for each system has been set to 0 eV in the plots.

In Figure 3, we show all the results for bent and linear CO_2 adsorption on Cu_x/TiO_2 (x=0-4) with a U value of 5.0 eV. The three characteristic localized peaks of linear CO_2 (at locations $\sim$ -9.7, -8.1, -4.5 eV in Cu_x/TiO_2) are preserved

regardless of Cu cluster, although the peaks are slightly shifted up in energy over pure TiO_2. Similarly, for bent CO_2, the delocalized character of the CO_2 peaks are preserved for bent CO_2 on TiO_2 with and without Cu clusters present. On the pure TiO_2 surface, the linear and bent CO_2 states extend within the valence band down to $\sim$ -9 eV. In the presence of Cu, the CO_2 states are pushed to lower energies extending up to -11 eV (see for example Bent CO_2 on Cu1). As mentioned in the main text, we consistently find strong hybridization between bent CO_2 and Cu states in the valence band as indicated by the overlap of delocalized Cu and bent CO_2 states (between 0 and $\sim$ -8 eV). In contrast, the linear CO_2 states are localized between -4 and -6 eV indicating weak hybridization with the Cu states.

6 CO adsorption on Cu_x/TiO_2

The most stable CO adsorption sites on Cu_x/TiO_2 are shown in Figure S4. We found the most stable adsorption site for CO on Cu/TiO_2 to involve a linear O-C-Cu bond at the top site of Cu atom with an adsorption energy of -1.96 eV. The bond distance of C-Cu was found to be 1.82 Å. The Cu atom was displaced significantly upon CO adsorption (by 0.57Å).

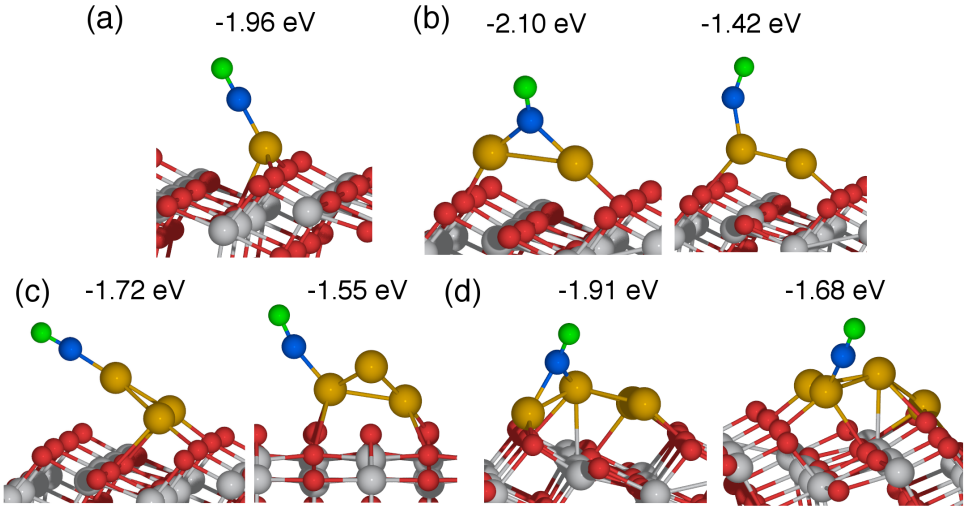

Figure S4: Most stable adsorption sites of CO on Cu_x/TiO_2 with x=1 (a), 2 (b), 3(c), and 4(I)(d). The numbers above each structure correspond to the adsorption energy of CO for that structure. Color scheme of atoms are the same as in previous Figures.

When CO adsorbs on Cu_2/TiO_2, the most stable site of adsorption was determined to be the bridge site where the C atom bonds with both Cu atoms and has an adsorption energy of -2.10 eV (see 4). This adsorption energy is also the largest among the CO adsorption energies over all Cu_x/TiO_2. The strong adsorption energy for Cu_2 again indicates the reactive nature of the Cu dimer, as was observed for CO_2 adsorption. The bond distances of both C-Cu bonds were 1.89Å. Adsorption of CO at the bridge site also results in the Cu-Cu bond distance to elongate from 2.30Å to 2.80Å. We also show the next most stable top site adsorption configuration on Cu_2/TiO_2 in Figure S4b. CO was found to be non-linearly bonded (the bond angle of Cu-C-O was 151°) with an adsorption energy of -1.42 eV. Adsorption of CO at the top site is significantly less stable than when CO adsorbs at the bridge site.

We adsorbed CO on several different adsorption sites over Cu_3/TiO_2. In the most stable configuration CO binds to the top Cu atom. The C-Cu bond distance was found to be 1.85Å and the adsorption energy was -1.72 eV. The next most stable adsorption site had an adsorption energy of -1.55 eV where CO bonded to a Cu atom that interacted with the surface. Several adsorption sites were tested for CO adsorption on $Cu_4(I)/TiO_2$, and the two most stable sites are shown in Figure 4d. The most stable adsorption site involved CO bridging between Cu_a and Cu_d atoms with a C-Cu bond distance of 1.92 and 1.97 Å, respectively. The next stable adsorption site consisted of CO adsorbing on top of a Cu_c atom with a C-Cu bond distance of 1.84 Å. This configuration had an adsorption energy of 1.68 eV. It was also found that CO adsorption in the top configuration bonded to any other Cu atom of $Cu_4(I)/TiO_2$ had adsorption energies between -1.57 to -1.68 eV.

7 Determining the Oxidation State of Cu using DDEC6

Table S6: DDEC6 charges (in electrons) for Cu^{2+} and Cu^{1+} complexes, as well as CuF/CuF_2 and CuO/Cu_2O (bulk and molecule).

Species	DDEC6 charge
Cu^{1+}	
Cu-CN-$(H_2O)_3$	0.33
Cu-Cl-$(H_2O)_3$	0.35
Cu-OH-$(H_2O)_3$	0.29
Cu-F-$(H_2O)_3$	0.41
Cu-CN-$(NH_3)_3$	0.25
Cu-Cl-$(NH_3)_3$	0.30
Cu-OH-$(NH_3)_3$	0.27
Cu-F-$(NH_3)_3$	0.30
Cu-CN-$(N_2)_3$	0.34
Cu-Cl-$(N_2)_3$	0.42
Cu-OH-$(N_2)_3$	0.46
Cu-F-$(N_2)_3$	0.52
Cu_2O (bulk)	0.33
Cu_2O (molecule)	0.28
CuF	0.50
Cu^{2+}	
Cu-$(CN)_2$-$(H_2O)_4$	0.78
Cu-Cl_2-$(H_2O)_4$	0.95
Cu-$(OH)_2$-$(H_2O)_4$	1.02
Cu-F_2-$(H_2O)_4$	1.10
Cu-$(CN)_2$-$(NH_3)_4$	0.67
Cu-Cl_2-$(NH_3)_4$	0.85
Cu-$(OH)_2$-$(NH_3)_4$	0.85
Cu-F_2-$(NH_3)_4$	1.01
Cu-$(CN)_2$-$(N_2)_4$	0.68
Cu-Cl_2-$(N_2)_4$	0.83
Cu-$(OH)_2$-$(N_2)_4$	0.67
Cu-F_2-$(N_2)_4$	1.02
CuO (bulk)	0.94
CuO (molecule)	0.44
CuF_2	0.93

We used DDEC6 charge analysis to calculate oxidation states of Cu. In order to identify the Cu states, we modeled several known Cu^{1+} and Cu^{2+} complexes. The geometries of Cu^{2+} (or Cu^{1+}) coordination complexes are known to adopt an octahedral (or tetrahedral) coordination with Cu at the center of these complexes.[25] For both complexes we considered several anionic and neutral ligands in different combinations. The neutral ligands considered were dinitrogen (N_2), water, and ammonia, while anionic ligands considered were Cl, F, CN, and OH. In octahedral complexes, out of the six vertices (four equatorial and two axial), two equatorial sites contained the anionic ligands for describing Cu^{2+} species with the rest of the four sites occupied by neutral ligands. In the case of the tetrahedral complexes, one of the four vertices contained an anionic ligand and other three contained a neutral ligand. The calculated DDEC6 charges are shown in Table S6. Besides these Cu coordination complexes, we also considered other systems such as CuO (bulk and molecule), Cu_2O (bulk and molecule), molecular CuF, and molecular CuF_2. We determined average DDEC6 charges for Cu in the various formal oxidation states. For the Cu^{2+} species the average DDEC6 charge was 0.85 with a standard deviation of 0.17, while for the Cu^{1+} species the average DDEC6 charge was 0.36 with a standard deviation of 0.08. The range of DDEC6 charges for Cu^{2+} was 0.44 to 1.10, while the range of charges for Cu+ was 0.25 to 0.52.

8 Diffusion of Adsorbed Cu Atoms

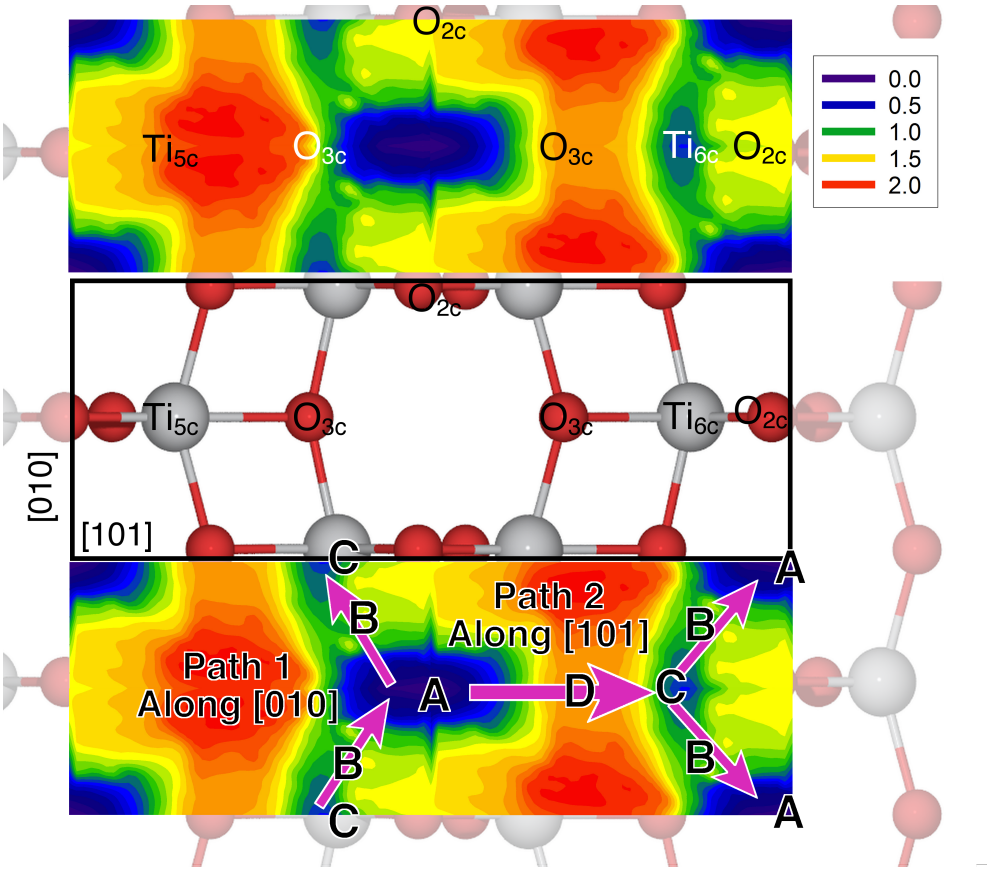

Figure S5: Potential energy surface for Cu adsorbed on the TiO_2 anatase(101). The contour of the energy surface is shown in the top panel and the corresponding top view of the TiO_2 surface is indicated by the black box in the middle panel. The minimum energy pathway is shown in the bottom panel along [010] and [101] directions through sites A/B/C/B/A and A/D/C/B/A respectively. For clarity only the top layer of the TiO_2 surface slab is shown. Surface atoms on the top and middle panels are labeled. The contour legend shows the relative energies compared to most stable adsorption site in eV.

Cu2 was found to stabilize CO_2 very strongly, but questions remain on its stability. We found the Cu2 formation energy to be 0.94 eV (2 $Cu/TiO_2 \longrightarrow Cu_2/TiO_2 + TiO_2$). We also calculated the potential energy surface of a Cu atom bound to the anatase (101) surface, as shown in Figure 5, in order to understand Cu diffusion on the surface. Cu diffusion is necessary for lone Cu atoms to form dimers. We adsorbed a Cu atom at different points on the surface by freezing the x- and y-coordinates of the Cu atom while allowing the z-coordinate of the Cu atom to relax. The bottom four O-Ti-O layers (192 atoms) of the surface slab were also frozen. The Cu atom was placed at different points on the surface with a spacing of 0.2Å between points. After considering the surface symmetry, we modeled a total of 263 geometries. Test calculations showed that freezing the bottom four and two layers produced results that were very comparable. The largest difference in energy between freezing four and two layers for the adsorption of Cu at different sites (e.g. bridge site between O_{2c} atoms or top sites was <0.13 eV).

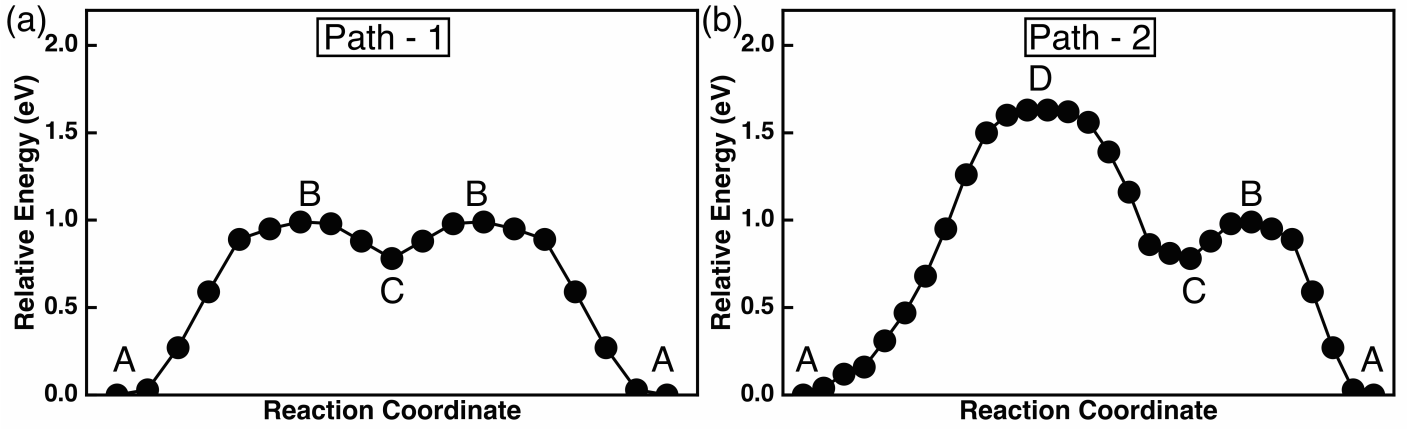

Figure S6: Diffusion barriers for Cu along Path 1 and Path 2 (shown in Figure S5 over the TiO_2 anatase(101) surface.)

The most stable site for Cu adsorption was at the bridge site between two O_{2c} atoms (indicated as point A in the bottom plot of Figure S5), which corresponds to the deepest energy well with an adsorption energy of -2.60 eV. The energy corresponding to this site represents the zero energy reference in the contour plots. The second most stable site of adsorption (site C) is at a top site above a Ti_{6c} atom, whose energy is 0.78 eV higher in energy than the most stable adsorption site A. In order for an atom to diffuse from a site A to another site A, it can follow one of the pathways indicated in the bottom plot of Figure S5. Path 1 moves along the [010] direction and follows the pathway indicated: A $\longrightarrow$ B $\longrightarrow$ C $\longrightarrow$ B $\longrightarrow$ A. The energy barrier for Path I was calculated to be 0.99 eV as the atom crossed from site A to site B (see Figure S6). Path 2 along moves in a general [101] direction and follows the indicated pathway: A $\longrightarrow$ D $\longrightarrow$ C $\longrightarrow$ B $\longrightarrow$ A. The energy barrier for Cu diffusion along this direction moves from site A to site D with an activation barrier of 1.63 eV. The lowest barrier for diffusion moves along the [010] direction with a value of 0.99 eV, which would indicate that Cu diffusion along the (101) surface should be relatively slow.

References

[1] N. G. Limas and T. A. Manz, *RSC Adv.*, 2016, **6**, 45727–45747.

[2] T. A. Manz and D. S. Sholl, *J. Chem. Theory Comput.*, 2010, **6**, 2455–2468.

[3] D. Koch and S. Manzhos, *J. Phys. Chem. Letters*, 2017, **8**, 1593–1598.

[4] R. F. Bader, *Atoms in molecules: a quantum theory*, 1990.

[5] G. Henkelman, A. Arnaldsson and H. Jónsson, *Comput. Mater. Sci.*, 2006, **36**, 354–360.

[6] G. Kresse and J. Furthmüller, *Phys. Rev. B*, 1996, **54**, 11169–11186.

[7] G. Kresse and J. Furthmüller, *Comput. Mater. Sci.*, 1996, **6**, 15–50.

[8] T. Shimanouchi, *Natl. Bur. Stand.*, 1972.

[9] G. Ramis, G. Busca and V. Lorenzelli, *Mater. Chem. Phys.*, 1991, **29**, 425–435.

[10] L. Mino, G. Spoto and A. M. Ferrari, *J. Phys. Chem. C*, 2014, **118**, 25016–25026.

[11] H. Y. T. Chen, S. Tosoni and G. Pacchioni, *Surf. Sci.*, 2016, **652**, 163–171.

[12] D. C. Sorescu, W. A. Al-Saidi and K. D. Jordan, *J. Chem. Phys.*, 2011, **135**, 124701.

[13] G. Pacchioni, *J. Chem. Phys.*, 2008, **128**, 182505.

[14] M. Capdevila-Cortada, Z. Łodziana and N. López, *ACS Catal.*, 2016, **6**, 8370–8379.

[15] N. A. Deskins, R. Rousseau and M. Dupuis, *J. Phys. Chem. C*, 2010, **114**, 5891–5897.

[16] Y. G. Wang, Y. Yoon, V. A. Glezakou, J. Li and R. Rousseau, *J. Am. Chem. Soc.*, 2013, **135**, 10673–10683.

[17] J. C. Garcia and N. A. Deskins, *J. Phys. Chem. C*, 2012, **116**, 16573–16581.

[18] H. He, P. Zapol and L. a. Curtiss, *Energy Environ. Sci.*, 2012, **5**, 6196.

[19] Y. G. Wang, D. C. Cantu, M. S. Lee, J. Li, V. A. Glezakou and R. Rousseau, *J. Am. Chem. Soc.*, 2016, **138**, 10467–10476.

[20] Y. Wang, S. Lany, J. Ghanbaja, Y. Fagot-Revurat, Y. P. Chen, F. Soldera, D. Horwat, F. Mücklich and J. F. Pierson, *Phys. Rev. B*, 2016, **94**, 245418.

[21] M. Heinemann, B. Eifert and C. Heiliger, *Phys. Rev. B - Condensed Matter and Materials Physics*, 2013, **87**, 3–7.

[22] D. O. Scanlon, B. J. Morgan and G. W. Watson, *J. Chem. Phys.*, 2009, **131**, 124703.

[23] N. Seriani, C. Pinilla and Y. Crespo, *J. Phys. Chem. C*, 2015, **119**, 6696–6702.

[24] Y. Yan, Y. Yu, S. Huang, Y. Yang, X. Yang, S. Yin and Y. Cao, *J. Phys. Chem. C*, 2017, **121**, 1089–1098.

[25] D. B. Rorabacher, *Chem. Rev.*, 2004, **104**, 651–698.